Anal. Chem. **2002,** *74,* 177−184

Toward a Fully Integrated Positive-Pressure Driven Microfabricated Liquid Analyzer

Paul G. Vahey, Sean A. Smith, Colin D. Costin, Younan Xia, Anatol Brodsky, Lloyd W. Burgess, and Robert E. Synovec*

Center for Process Analytical Chemistry (CPAC), Department of Chemistry, Box 351700, University of Washington, Seattle, Washington 98195-1700

A versatile integrated analyzer with a flow-programmed injection strategy and multiwavelength detection is described with applications toward sampling, flow injection analysis, and capillary separations. Continuous near-real-time sampling is a major benefit of the flow-programmed injection technique. Injection volumes ranging from 250 pL to several microliters were made without electrophoretic flow. Multiwavelength grating light reflection spectroscopy (GLRS) and transmission absorbance spectroscopy were performed simultaneously in a detection volume of 150 pL. The utility of these detection methods for refractive index (RI) and absorbance detection in capillary channels is demonstrated through analysis of salt, indicator, and dyes. GLRS is a unique, selective, and path-length-independent technique for probing RI, absorbance, and other optical properties. A limit of detection (LOD) of 170 μM was achieved for GLRS interferometric detection of FD&C Red #3, which corresponded to 2.6 fmol of analyte in the 150-pL detection volume. A LOD of 2 mM for phosphate buffer, or 3 fmol in the 150-pL detection volume will also be demonstrated. A siloxane coating on the GLRS grating was employed as a sensing layer to probe interactions between the sample and stationary phase. The combined GLRS interferometric response provided insight into both optical and chromatographic properties of samples. Open tubular capillary liquid chromatography with multidimensional multiwavelength detection is demonstrated for the analysis of three food dyes. Separation efficiency, *N*, of 16 000 was achieved for an unretained dye peak eluting at 12 min. Integration of novel sampling and detection schemes makes this a broadly applicable liquid analyzer.

Miniaturization of conventional laboratory instrumentation has been at the center of much research and development over the past 15 years.[1] Microfabricated devices for the manipulation and analysis of liquids have been used to increase the amount of information with respect to sample size, time, cost, and throughput. Micrototal analysis systems (μ-TAS) are intended to combine all steps of a complete chemical analysis on a single integrated device[2,3] to provide efficient conversion of chemical information to electronic information.[4] Miniaturization has helped to bring about surges in the fields of DNA sequencing,[5,6] high-throughput screening,[7] and proteomics,[8,9] as well as the analysis of amino acids[10,11] and enzymes.[12]

Most detection schemes in these μ-TAS have been based on absorbance or fluorescence. Traditional absorbance is compromised in microfabricated systems, because it is difficult to achieve sufficient path length in small volumes. Limits of detection (LOD) are rarely below 0.1 mM for chip-scale absorbance detection.[13,14] Some researchers have attempted to increase sample path lengths through novel channel configurations[15,16] and waveguiding materials.[14,17] Fluorescence has been used to increase signal-to-noise ratios. Some researchers have reported detection of single molecules using laser-induced fluorescence.[11,18] Although fluorescence improves sensitivity, it is only applicable for analytes that fluoresce naturally or analytes that have been derivatized to fluoresce. Other developments in chip-based detection include surface plasmon resonance (SPR),[19,20] electrical conductivity,[21]

(1) Figeys, D.; Pinto, D. *Anal. Chem.* **2000**, *72*, 330A−335A.
(2) Harrison, D. J., van den Berg, A., Eds. *Proceedings of the μ-TAS '98 Workshop*; Kluwer Academic: Dordrecht, 1998.
(3) Burggraf, N.; Krattiger, B.; de Mello, A. J.; de Rooij, N. F.; Manz, A. *Analyst* **1998**, *123*, 1443−1447.
(4) Manz, A.; Graber, N.; Widmer, H. M. *Sensors Actuators* **1990**, *B1*, 244−248.
(5) Schmalzing, D.; Adourian, A.; Koutny, L.; Ziaugra, L.; Matsudaira, P.; Erlich, D. *Anal. Chem.* **1998**, *70*, 2303−2310.
(6) Wooley, A. T.; Mathies, R. A. *Anal. Chem.* **1995**, *67*, 3676−3680.
(7) Freemantle, M. In *Chem. Eng. News* **1999**, *77*, 27−36.
(8) Li, J.; Thibault, P.; Bings, N. H.; Skinner, C. D.; Wang, C.; Coyler, C.; Harrison, J. D. *Anal. Chem.* **1999**, *71*, 3036−3045.
(9) Borman, S. In *Chem. Eng. News* **2000**, *78*, 31−37.
(10) Liu, S.; Shi, Y.; Ja, W. W.; Mathies, R. A. *Anal. Chem.* **1999**, *71*, 566−573.
(11) Haab, B. B.; Mathies, R. A. *Anal. Chem.* **1999**, *71*, 5137−5145.
(12) Hadd, A. G.; Jacobson, S. C.; Ramsey, J. M. *Anal. Chem.* **1999**, *71*, 5206−5212.
(13) Vahey, P. G.; Park, S. H.; Marquardt, B. J.; Xia, Y.; Burgess, L. W.; Synovec, R. E. *Talanta* **2000**, *51*, 1205−1212.
(14) Puyol, M.; del Valle, M.; Garces, I.; Villuindas, F.; Dominguez, C.; Alonso, J. *Anal. Chem.* **1999**, *71*, 5037−5044.
(15) Renn, C. N.; Synovec, R. E. *J. Chromatogr. A* **1991**, *536*, 289−301.
(16) Hancock, D. O.; Renn, C. N.; Synovec, R. E. *Anal. Chem.* **1990**, *62*, 2442−2447.
(17) Veldhuis, G. J.; Lambeck, P. V. *Appl. Phys. Lett.* **1997**, *71*, 2895−2897.
(18) Fister, J. C.; Jacobson, S. C.; Davis, L. M.; Ramsey, J. M. *Anal. Chem.* **1998**, *70*, 431−437.
(19) Berger, C. E. G.; Beumer, T. A. M.; Kooyman, R. P. H.; Greve, J. *Anal. Chem.* **1998**, *70*, 703−706.
(20) Sota, H.; Hasegawa, Y. *Anal. Chem.* **1998**, *70*, 2019−2024.
(21) Zeemann, A. H.; Schnell, E.; Volgger, D.; Bonn, G. K. *Anal. Chem.* **1998**, *70*, 563−567.

10.1021/ac010440o CCC: $22.00
Published on Web 11/22/2001

thermal conductivity,[22] chemiluminescence,[23] and electrochemical methods,[24,25] including ion-selective electrodes.[26]

Although many detection techniques have been explored, the need still exists for an inexpensive, simple, universal, and path-length-independent detection method. Refractive index (RI) detection is widely used for detection in the analysis of polymers, sugars, biomolecules, particle sizing, and other solutes that lack chromophores, and fluorophores. Simple cost-effective equipment is among the many advantages of RI detection. RI has been proven to be nondestructive, compatible with a wide variety of buffers, and universal in nature for the determination of analytes at micromolar to millimolar concentrations.[3] RI can complement other detection techniques, thereby increasing the dimensionality of chip-scale detection. Waveguides have been incorporated into flow channels to increase RI sensitivity. An on-chip Mach−Zender interferometer with a sensitivity of 7×10^{-5} RIU was developed, but no attempts were made to interface the detector with a dynamic or capillary-scale sampling device.[27] A silicon micromachined spiral-shaped refractometer sensitive to 10^{-5} RIU has been reported in which light remained in the waveguiding structure within a certain radius, depending upon the RI contrast between sample and waveguide.[17] Other researchers developed a mode-filtered detection cell by inserting a fiber-optic into a glass capillary and flowing sample between the two.[28] A change in the refractive index of the cladding as small as 3×10^{-6} RIU was sufficient to allow light to escape radially. In the mode-filtered system, chromatographic stationary phase was substituted for the fiber-optic cladding, creating an annular column, which added a degree of selectivity to the detector.[29] Analytes partitioned into the stationary phase/cladding, where they were concentrated as much as 600-fold, resulting in a LOD of 500 ppb for cumene in water. These elegant detection systems offer insights into the interaction between sample and waveguide; unfortunately, their detection volumes were in the tens of nanoliters, which is too large for efficient detection in chip-based separation systems. Modified surfaces have been used to increase the selectivity and sensitivity of detectors for SPR[19,20] and interferometry.[30] An SPR multisensor was made that incorporated an array of immobilized antibodies for multichannel immunoassays.[19] Modifying a gold surface with *Escherichia coli* resulted in a stable and reusable SPR sensor used to monitor conformational changes in proteins over a pH range of 0.12−7.8.[20] Appropriately derivatized porous silica was used in an optical interferometer with picomolar sensitivity.[30] This interferometric sensor was hindered by slow reaction kinetics between receptors bonded to the silica and analytes. Although each of these techniques was sensitive and highly selective, tradeoffs included elaborate surface modifications, and the detection methods were not universal. An elegant interferometer was interfaced with CE via a holographic optical element that split the incident laser into two coherent beams laterally spaced 14 μm apart and focused them in the plane of the channel.[3] One beam probed the capillary channel, and the second was directed through the glass wafer and used as a reference. The two beams diverged in the far field creating an interference pattern, which was used to obtain an LOD of 10 mM for carbohydrates, or roughly 5×10^{-4} RIU, with 16-pL injections. Although thermal noise caused low sensitivity, the authors claimed that the technique holds promise, because microfabricated channels have low thermal mass, allowing temperature control.[3] Recent work demonstrated that sensitivity of on-chip techniques could be increased using multipass detection cells.[31] An etched channel with hemispherical sidewalls and two flat faces produced fringing in backscattered light when it was exposed to an unfocused collimated beam. Using nonflowing samples, conditions were optimized to achieve detection limits of 0.7 mM for glycerol, or a sensitivity of 9.7×10^{-6} RIU in a volume of 188 pL.[31]

Grating light reflection spectroscopy (GLRS) has been demonstrated as a unique and selective technique for probing changes in both the real and imaginary portion of the optical dielectric permittivity of a sample.[32,33] GLRS is a technique that monitors light reflected from a transmission, diffraction grating in contact with a sample.[32] Unlike other techniques that exploit optical reflection phenomena, GLRS relies upon not simply the attenuation of the sampling beam, but on the loss of coherence of the penetrating evanescent wave relative to the wave that originates at the grating. When the incident beam fulfills necessary conditions, a singularity wavelength in a transmitted diffracted order is transformed from a traveling wave transmitted through the bulk medium to an evanescent wave that penetrates into the sample. Near these critical transitions, the reflected light characteristics in all of the orders display a singular behavior that is relatively simple to observe and interpret.[34] GLRS provides information on interactions at the grating−sample interface as well as probes the bulk properties of the sample.[33] The resulting signal is a combination of responses based on RI and absorbance that has been demonstrated in the analysis of dyes, alcohols,[35] aromatic hydrocarbons,[36] polystyrene microspheres,[32] and dendrimers.[34] Because GLRS is a reflection-based measurement, it is concentration-dependent and path-length-independent, making it a desirable detection technique for μ-TAS. Sensitivity in terms of the real part of the optical dielectric permittivity of a sample (refractive index) has been demonstrated to be on the order of 2×10^{-6} RIU, depending on the detection system resolution.

The research presented here reflects an effort to develop sampling, separation, and detection toward well-integrated and

(22) Terry, S. C.; Jerman, J. H.; Angell, J. B. *IEEE Trans. Electron Devices* **1979**, *26*, 1880−1891.
(23) Arora, A.; de Mello, A. J.; Manz, A. *Anal. Comm.* **1997**, *34*, 393−395.
(24) Woolley, A. T.; Lao, K.; Glazer, A. N.; Mathies, R. A. *Anal. Chem.* **1998**, *70*, 684−688.
(25) Wang, J.; Tian, B.; Sahlin, E. *Anal. Chem.* **1999**, *71*, 5436−5440.
(26) Linder, E.; Buck, R. P. *Anal. Chem.* **2000**, *72*, 336A−342A.
(27) Heideman, R. G.; Veldhuis, G. J.; Jager, E. W. H.; Lambeck, P. V. *Sensors Actuators B* **1996**, *35−36*, 234−240.
(28) Synovec, R. E.; Sulya, A. W.; Burgess, L. W.; Foster, M. D.; Bruckner, C. A. *Anal. Chem.* **1995**, *67*, 473−482.
(29) Foster, M. D.; Synovec, R. E. *Anal. Chem.* **1996**, *68*, 1456−1463.
(30) Lin, V. S.-Y.; Motesharei, K.; Dancil, K. S.; Sailor, M. J.; Ghadiri, M. R. *Science* **1997**, *278*, 840.
(31) Swinney, K.; Markov, D.; Bornhop, D. *Anal. Chem.* **2000**, *72*, 2690−2695.
(32) Brodsky, A. M.; Smith, S. A.; Burgess, L. W. *Appl. Spectrosc.* **1998**, *52*, 332A−343A.
(33) Anderson, B. B.; Brodsky, A. M.; Burgess, L. W. *Anal. Chem.* **1996**, *68*, 1081−1088.
(34) Smith, S. A.; Vahey, P. G.; Brodsky, A. M.; Burgess, L. W. *Anal. Chem.* **2000**, *72*, 4428−4434.
(35) Anderson, B. B.; Brodsky, A. M.; Burgess, L. W. *Phys. Rev. E* **1996**, *54*, 912−923.
(36) Kelly, M. J.; Sweatt, W. C.; Kemme, S. A.; Kasunic, K. J.; Blair, D. S.; Zaidi, S. H.; McNeil, J. R.; Burgess, L. W.; Brodsky, A. M.; Smith, S. A. Sandia National Laboratories: Albuquerque, 2000, pp 1−35.

inexpensive μ-TAS, including on-chip multivariate detection schemes such as GLRS. Sample injection and handling have played and will continue to play an important role in any μ-TAS. Any separation method must implement a reproducible sample injection scheme to provide dependable, quantitative information. It has been well-documented for microfabricated open tubular liquid chromatography (OTLC) that very small sample injection schemes must be used to maintain column efficiency, which can be lost by sample overloading. The idea of μ-TAS also requires that these injection schemes be developed so that they can be easily integrated onto the chip with the separation and detection mechanisms. A unique aspect of these analyzers involves the capability to make subnanoliter injections through flow-programming without using electrophoretic flow.[13] Here, we report flow-programmed, near-real-time, on-chip sampling as a viable injection strategy. Injection reproducibility has been improved through automation and will be demonstrated. Building upon recent work involving microfabricated liquid chromatographs[13] and GLRS measurements in flow-through microfabricated detection cells,[34] gratings were incorporated into channels of suitable dimension for chromatographic separations. A submicrometer coat of siloxane was used on the grating to promote adhesion and may have acted as a sensing layer to probe interactions between samples and the PDMS stationary phase. Developments in detection included interferometric fringes that were observed in the GLRS signal in addition to the expected singular wavelength. The combined GLRS−interferometric response corresponded to optical as well as chromatographic characteristics of analytes. The detection aspect of this work differs from previously reported RI-related detection methods in several ways. First, GLRS is not simply RI detection, offering multivariate information. Second, the incident light in these experiments was collimated white light, whereas most other techniques have incorporated monochromatic light.[3,15,28,31,37−39] Third, the fringes were observed in wavelength space, as opposed to a physical fringe pattern.[3,31] Periodic behavior in our data conveyed redistribution of energy within a collimated beam. Fourth, it will be shown that the fringe pattern, like the GLRS singularity, was a phenomenon tied to the optical grating. And finally, multiwavelength absorbance detection can be incorporated simultaneously into the device to complement the GLRS detection. In this manner, we capitalized on a major advantage of μ-TAS, which is the ability to microfabricate multiple components into a single system.[7]

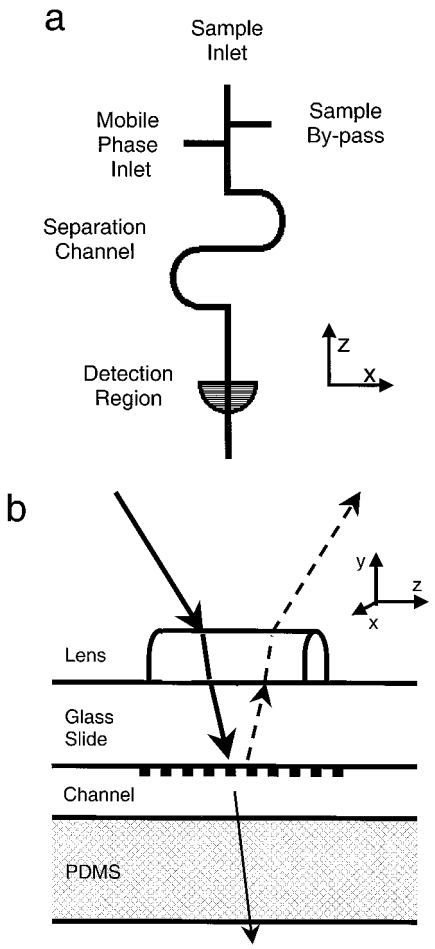

Figure 1. (a) Instrument diagram: microfabricated liquid analyzer viewed from the top. A chrome grating was incorporated into the channel wall for GLRS detection. (b) Absorbance: GLRS detection cell, not drawn to scale. Incident white light was focused through a semicylindrical lens onto the back of the chromium grating. The lens focused light to a spot ≥100 μm in the *x* dimension, but the 150-μm *z* dimension of the light was not affected. The detection cell volume was, therefore, 100 × 10 × 150 μm, or 150 pL. The first reflected order was used for GLRS data. One-half of the incident beam passed through the chromium oxide grating into the flow channel and was used for transmission measurements.

EXPERIMENTAL SECTION

Microfabrication. Channels of dimensions 10 × 100 μm, as shown in Figure 1a, were fabricated in PDMS using soft lithography, a rapid and low-cost prototyping method for microfabrication.[40,41] The masters for the microchannels were designed on a computer using Freehand 7.0 software (Macromedia Inc., San Francisco, CA). The pattern of the OTLC analyzer is shown in Figure 1a. Images were printed on a transparency using a high-resolution printer at 2560 dpi. AZ 4620 photoresist (Hoechst Celanese Corp., Somerville, NJ) was spin-coated onto 3-in. silicon wafers (Silicon Sense, Nashua, NH) to a thickness of 10.0 ± 0.4 μm, measured on the masters only using an Alpha-Step 100 profilometer (Tencor Instruments, Mountain View, CA). The channel patterns were then transferred into the photoresist using collimated UV light, and excess photoresist was removed using AZ 351 developer (Clariant Corp., Somerville, NJ).

The PDMS (Sylgard 184, Dow Corning, Midland, MI) was prepared, degassed, and poured over the channel master. After curing for 1 h at 65 °C, the PDMS was removed from the channel master, plasma-treated (Branson International Plasma Corp., Hayward, CA) to activate surface groups, and joined with a cleaned glass surface that had been activated in the same plasma. The channel dimensions of the PDMS constructs were not verified, but the subsequent performance of the PDMS channels is indicative that their dimensions were reasonably close to those of the master.

(37) Bornhop, D. J.; Dovichi, N. J. *Anal. Chem.* **1987**, *59*, 1632−1636.
(38) Bruno, A. E.; Krattiger, B.; Maystre, F.; Widmer, H. M. *Anal. Chem.* **1991**, *63*, 2689−2697.
(39) Synovec, R. E. *Anal. Chem.* **1987**, *59*, 2877−2884.
(40) Duffy, D. C.; McDonald, J. C.; Schueler, O. J. A.; Whitesides, G. M. *Anal. Chem.* **1998**, *70*, 4974−4984.
(41) Xia, Y.; Whitesides, G. M. *Angew. Chem., Int. Ed. Engl.* **1998**, *38*, 550−575.

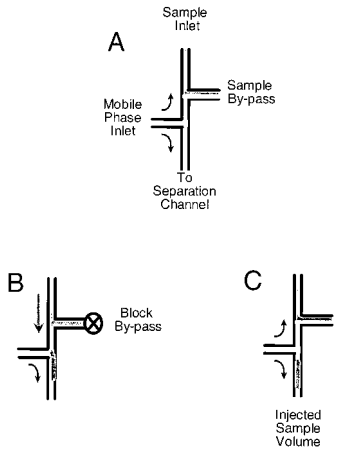

Figure 2. Flow-programmed injection scheme in which the mobile phase flows at 40 nL/min, and the sample flows at 20 nL/min: (A) default setting; (B) sample is injected by blocking the sample bypass channel, and the injection volume is controlled by the length of time the bypass is closed; (C) bypass is reopened, pushing the injected plug down the separation channel and returning the sample stream to the default setting.

Liquid reached the microfabricated channels through interconnects created in the PDMS by affixing glass posts to the master before pouring the elastomer. The posts were ground to an outer diameter slightly less than 1/16 in.. Once channels were formed by joining PDMS to the glass slide, PEEK tubing (Upchurch Scientific, Oak Harbor, WA), 0.010-in. i.d. × 1/16-in. o.d. was then glued into the holes left by the glass posts. Five-minute epoxy (Devcon Consumer Products, Danvers, MA) was sufficient for water matrixes, but H74F epoxy (Epo-Tek, Billica, MA) was required for buffered solutions, because the 5-min. epoxy did not hold up with the buffered solutions.

Sampling. Samples contained FD&C Blue #1 dye, FD&C Red #3 dye (H. Kohnstamm, New York, NY), Bromocresol green (Sigma-Aldrich, Milwaukee, WI), and Phenol Red (Sigma-Aldrich, Milwaukee, WI) dissolved in water. Two syringe pumps (μLC-500, Isco Inc., Lincoln, NE) were used to deliver the mobile phase, as well as the sample, to the analyzer, indicated by the inlets to the analyzer in Figure 2. With one of the two pumps, a 100-μL volume containing sample was introduced into the sample inlet of the OTLC analyzer using an injection valve (Rheodyne, 7125, Cotati, CA). This achieved pseudo-steady-state sample conditions for subsequent flow-programmed injection into the OTLC separation channel (Figure 2) without having to load the sample into one of the syringe pumps.

The sample and the mobile phase flowed continuously through the analyzer at all times. Low flow rates and small channel dimensions resulted in conditions of laminar flow within the PDMS channels.[42,43] Experimentally controlling the flow conditions such that the mobile phase was flowing at about twice the rate of the sample stream resulted in the desired default sampling conditions in which the sample stream was not diverted into the separation channel. For example, a 10 nL/min flow rate through the separation channel was achieved by applying a 40 nL/min flow rate into the mobile phase inlet coupled with a 20 nL/min flow rate into the sample inlet and then adjusting the height of a short section of capillary tubing connected to the OTLC "chip" outlet such that most of the flow exited by way of the sample bypass, that is, 50 nL/min. Although this experimental method of controlling flow rate is not ideal, the results to be presented will suggest that the injection strategy could be fully programmable if properly engineered. Figure 2 demonstrates the ability to isolate the separation channel from a continuously flowing sample stream. Bromocresol green was injected for the sampling studies because of the strong signal detected at 8 mM. Injections were achieved by closing a solenoid valve (Valcor Instruments, Springfield, NJ) so that the sample stream was temporarily redirected to the separation channel, as in Figure 2. A programmable function generator (Stanford Research Instruments, Sunnyvale, CA) was used to control the time actuation of the solenoid, which produced reproducible sample injection volumes. Valve actuation times were varied to introduce different injection volumes onto the channel for efficiency versus injection volume studies. For example, closing the valve for 2 s redirected the combined sample and mobile phase flow (60 nL/min) down the separation channel, thus producing a 2-nL injected sample volume. In the context of selecting the appropriate injection volume, the system is programmable. When the valve in the sample bypass was reopened, flow conditions returned to the default condition, that is, with the injected sample flowing through the separation channel.[13] Absorbance data was collected for the sampling studies using an Ocean Optics SD2000 to minimize any unknown effects from the GLRS detection scheme.

Detection. Figure 1b diagrams the detection cell used for simultaneous reflection and transmission spectroscopy. The incident beam was focused onto a metal (chromium)/dielectric transmission grating from which roughly half of the incident light was reflected. Reflected light carried rich information about the sample in the region of the "singularity" wavelength (λ), which occurs when the following condition is satisfied,

$$n_D - \sin\theta - \frac{m\lambda}{\Lambda} = 0 \qquad m = ..., -1, 0, +1, ... \qquad (1)$$

where n_D is the refractive index of the studied sample, θ is the incident angle oriented perpendicular to the grating lines, m is the transmitted diffraction order containing the critical wavelength, λ is the singular wavelength, and Λ is the grating interval. Within the critical, transmitted, diffraction order, the wavelength region to the long wavelength side of the singularity wavelength produced an evanescent field that penetrated into the sample in contact with the grating and interacted with the reflected light, producing a (GLRS) response. The wavelength at which the singularity occurs is a function of the sample refractive index. Intensity of the singularity corresponds to the degree of scattering or absorption of the evanescent field by the sample. In this system, the singularity for water was ~630 nm.

The process by which the diffraction gratings were fabricated has been described in previous work,[33] but will be summarized. The gratings were holographically formed on a chrome-coated substrate by exposing the interference pattern of an argon ion laser beam to a layer of photoresist material on the substrate, and then the chromium metal was wet chemically etched. This procedure resulted in transmission gratings with a square groove

(42) Bianchi, F.; Ferrigno, R.; Girault, H. H. *Anal. Chem.* **2000**, *72*, 1987−1993.
(43) Kamholz, A. E.; Weigl, B. H.; Finlayson, B. A.; Yeager, P. *Anal. Chem.* **1999**, *71*, 5340−5347.

profile and a 50% duty cycle. The particular grating used for these experiments was determined to have a period of 1095 nm, and a height of 100 nm.

To construct the optical train around the grating/channel interface, a Tungsten−halogen bulb serving as the broadband light source was coupled through a 100-μm core fiber-optic and collimated. This light was then passed through a polarizer to select the TM or *p*-polarized component. The resulting beam was reduced down through a 150 μm wide (in the *z* dimension) by 1 mm in the (*x* dimension) aperture before it was incident upon the grating substrate at an angle of 50°. This beam first passed through a cylindrical lens of 2.5 mm back focal length in order to focus the beam to ≥100 μm in the *x* dimension while maintaining collimation in the optical plane. The lens, incident beam angle, and grating substrate thickness were all chosen such that the focal point of the lens occurred at the grating/channel interface. Thus, the full intensity of the incident light reflected within the "window" defined by the microchannel width of 100 μm. The channel depth of 10 μm made the sampling volume for these experiments (0.1 × 0.15 × 0.01) mm^3 or 150 pL.

Roughly one-half of the incident beam was reflected off the grating and was recollimated by passing back through the cylindrical lens. This was coupled into a 200-μm core fiber-optic via a 10× microscope objective, which passed the reflected light into a McPherson 270 monochromator equipped with a Princeton Instruments 576e CCD camera for recording 576 point spectra from 606.1 to 660.7 nm at a resolution of 0.2 nm FHWM and 0.1 nm/pixel. This spectral window was chosen because the 1095-nm period grating used for this work resulted in a singularity at 630 nm for water, which served as the sample carrier stream.

Roughly one-half of the light was transmitted completely through the channel, then collected and recollimated by passing through a spherical lens. This light was coupled into a 400-μm core fiber-optic via a 10× objective, passing the reflected light into an Ocean Optics SD2000 spectrometer (Ocean Optics Inc., Dunedin, FL). A total of 2046 point spectra from 174.7 to 865 nm were produced at a resolution of 1.3 nm fwhm at 0.4 nm/pixel. The usable range of the optical system was limited by the light source, which has little illumination intensity below 370 nm. In one experiment, the fiber-optic carrying reflected light was plugged into the second channel of the Ocean Optics SD2000.

Flow in the PDMS channels was oriented perpendicular to the grating lines. The application of Prime Coat left a submicromolar siloxane residue on the glass and metal substrate (Figure 2b) that may have behaved as a sensing layer, increasing interaction capabilities at the grating−sample interface.

Data Analysis Procedure. Because of the complexity of the phenomena being measured, it is instructive to describe how the data were handled prior to plotting in graphical form. The raw signal data were manipulated using the following algorithm for subsequent interpretation. First, corrections were made for source fluctuations by normalizing each spectrum to "inactive" regions at the red end of each spectrum. Next, the background signal from the mobile phase $I_0(\lambda)$ was generated using the mean of 20 baseline spectra. Transmitted signals were calculated as absorbance spectra by the usual formula. Reflected, GLRS spectra were calculated as changes in reflectance from the water background.

$$\Delta \text{ Reflectance} = \left(\frac{I(\lambda) - I_0(\lambda)}{I_0(\lambda)}\right) \times 100\% \qquad (2)$$

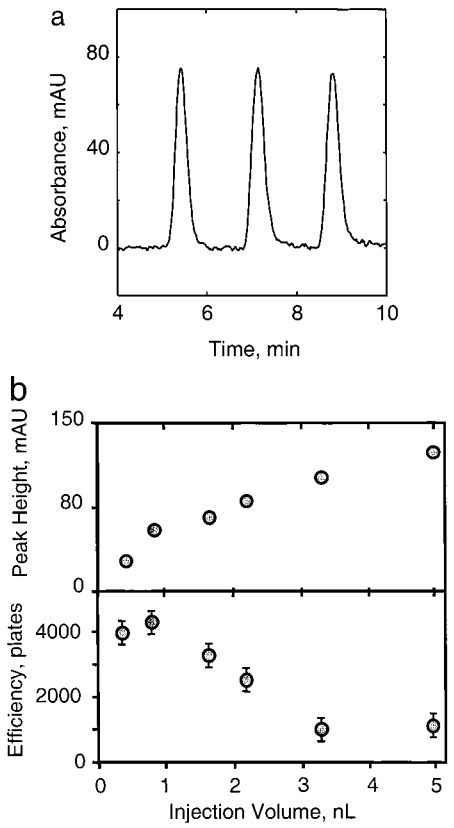

Figure 3. (a) Three injections of 8 mM Bromocresol green in 5 mM phosphate buffer, pH of 7. Injections shown using the scheme in Figure 2. Each injection was 2 s long, moderated by a programmable function generator, and injected onto a 10 μm × 100 μm × 23 cm microchannel fabricated into PDMS. The absorbance signal was collected on an Ocean Optics SD2000 absorbance detector. (b) Upper plot is peak height versus injection volume for 8 mM Bromocresol green in 5 mM phosphate buffer, pH of 7, and separation flow rate of 10 nL/min. Lower plot is efficiency, *N*, in plates versus injection volume for the same dye and separation channel flow rates.

RESULTS AND DISCUSSION

Analyzer Injection Reproducibility. The first study conducted was the test of injection reproducibility with the flow-programmed injection scheme. Figure 3a shows three consecutive injections that were made on the separation channel. Each of these injections is 2 nL and represents a 2-s time period during which the sample bypass valve was closed, forcing a sample plug into the separation channel. The implementation of the automated injection scheme produced adequate injection volume control and reproducibility. Using the programmable function generator with the solenoid valve, precision for volume injected with automation was found to be typically 3%, relative standard deviation of the peak height (0.03 nL/1 nL injection volume). The second part of our study involved examining the optimization of injection volume for chromatographic efficiency, and concentration at the detector. There are two plots shown in Figure 3b. The top plot is peak

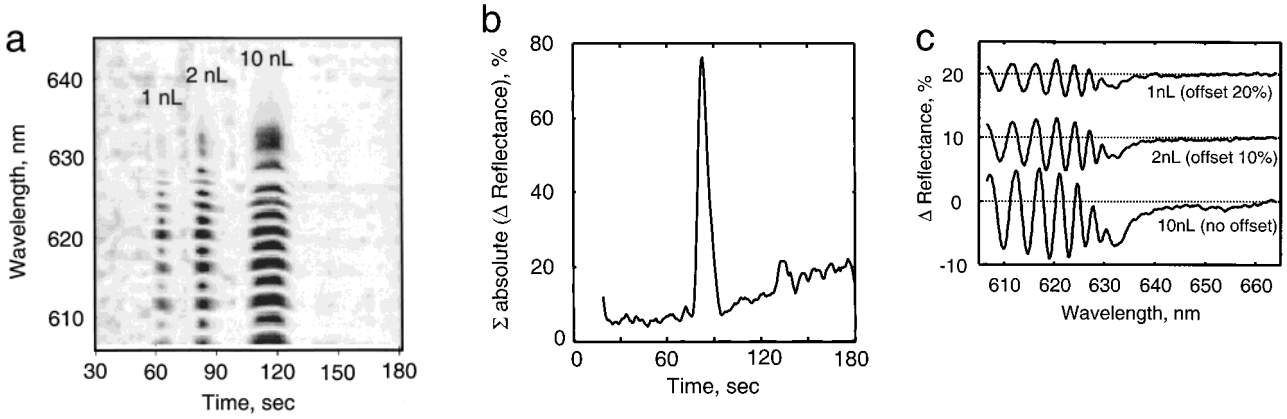

Figure 4. (a) Contour plots showing GLRS detection for three separate injections of 13.5 mM FD&C Red #3 in water with a water mobile phase flowing at 56 nL/min, in a PDMS channel 75 μm × 9.3 μm × 4.4 cm. Data were collected using a McPherson 270 monochromator and a Princeton Instruments 576 CCD camera. (b) Total GLRS signal obtained by summing absolute values in reflected spectra along the wavelength axis. This signal is obtained from the 2-nL injection. Total GLRS signals were used in calculating limits of detection. Absolute values were used to account for negative numbers in the fringe pattern. (c) Change in reflectance versus water (dotted lines) for three injections of the FD&C Red #3 injections. The injections are shown offset in steps of 10% Δreflectance from water.

height versus injection volume. As expected, these data indicate that the peak height is directly related to the injection volume. The peak height increases as the injection volume increases and appears to reach steady state concentrations as the injection volume reaches 5 nL. The lower plot in Figure 3b is chromatographic efficiency, *N*, in plates versus volume injected. These data clearly indicate the efficiency of the system has an optimal injection volume of <1 nL. It can also clearly be seen that as the injection volume increases over 1 nL, the efficiency of the system quickly decreases. Thus, the analyzer can be readily tuned to provide a compromised, yet optimum, detection sensitivity and efficiency (sample throughput) for a given application. This on-chip injection strategy may produce pressure fluctuations within the OTLC column and, thus, impact the separation efficiency and resolution. Further study is warranted.

GLRS Response. Studies of the GLRS spectral response in Figure 4 show trends related to sample properties, such as RI and adsorption onto or partitioning into the siloxanes in the detection cell. The potential information content of this multiwavelength interferometric−GLRS detection can be seen in data collected using the McPherson monochromator/Princeton Instruments CCD, shown in Figure 4a, showing three separate injections of 13.5 mM FD&C Red #3 in water with a water mobile phase. Injection volume affected concentration at the detector, as shown in Figure 4. In addition to the singularity, periodic behavior was observed in the reflected signal. The apparent "fringing" was present within a collimated beam of light, appearing only in wavelength space, as opposed to physical fringes that could be viewed as light and dark patches within an interference pattern. This periodicity was obviously the result of transmitted light reflecting at PDMS−sample interfaces within the channel and interacting with the GLRS phenomenon. Previous experiments with an identical optical train probing larger channels (400 × 50 μm) did not generate fringes.[34] As in backscatter interferometry, overfilling the channel with incident light was likely a necessity for generating fringes. Chromatographic peaks with GLRS detection were more clearly seen after summing the absolute values of reflected spectra along the wavelength axis, resulting in total signal chromatograms Figure 4b. As such, the device could provide continuous near-real-time sampling at a rate of 180 samples/h. A 2-nL injection volume (with a standard deviation of 0.06 nL) of 13.5 mM FD&C Red #3 eluted with a peak concentration of 3.9 mM, and a S/N of 68 in the total signal chromatogram. Noise, or σ, was the standard deviation of the baseline signal in a time window at least as wide as the chromatographic peak, in a region without sample. The 3σ LOD for this compound was 170 μM, or 2.6 fmol of analyte in the 150-pL detection volume. Analysis of spectra from the apex (concentration maximum) of each injected peak, Figure 4c, revealed how sample properties and concentration affected several features of this augmented GLRS response. GLRS features observed in Figure 4c include fringe amplitude, offset from the water background, fringe frequency, fringe phase offset, singularity wavelength, width of singularity, relative size of singularity to fringes, and return of signal back to water background on the red side of the singularity. Analyte characteristics affecting the fringes included refractive index, optical absorption, ionic strength, and dynamics of adsorption or partitioning into the channel walls. Given that FD&C Red #3 has a very low absorptivity in the spectral window of this GLRS system, the properties measured were probably RI and interaction between the retained dye and PDMS in the channel walls and coated on the grating. The spectral peak of the singularity, seen in Figure 4c at 632 nm, broadened for light-absorbing compounds and analytes partitioning into the siloxane coat on the grating. The amplitudes of the singularity and the fringes increased with concentration. Fringes were red-shifted in more concentrated samples, corresponding to a higher RI. The negative slope of the baseline through the fringes before the singularity and shallow slope of the signal returning to baseline after the singularity were also characteristic of light-absorbing compounds and analytes at the grating and effectively changing the broad band reflectivity coefficient at the grating interface. At this stage, we cannot deconvolute the effect on the GLRS signal due to partitioned analyte versus analyte within the mobile phase.

GLRS spectra of sodium chloride solutions were analyzed using the Ocean Optics spectrophotometer as shown in Figure 5a. The Ocean Optics spectrophotometer had a spectral window in these experiments of 370 nm to 820 nm, which was limited by the output

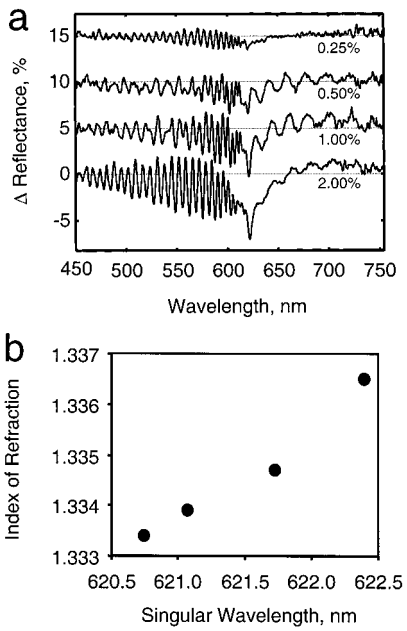

Figure 5. (a) Change in reflectance versus water (dotted lines) for four sodium chloride injections. Samples were 0.25, 0.50, 1.00, and 2.00% (by weight) NaCl in water. Samples are shown offset in steps of 5% Δreflectance from water. Data were collected using an Ocean Optics SD2000 diode array spectrophotometer. (b) Calibration plot for RI versus singular wavelength. Sodium chloride was used to demonstrate the sensitivity of the singular wavelength to sample RI. Each nanometer shift of the singularity corresponded to a ΔRI of 0.0018.

of the white light source, compared to the 55-nm window of the McPherson monochromator. Although the McPherson could provide better resolution and the liquid nitrogen cooled CCD achieved higher S/N, distinct advantages of obtaining a broader spectrum became apparent. Using eq 1 with the current optical configuration, a spectral window of 55 nm allows one to view a ΔRI of 0.050 RIU, whereas a 450-nm window would permit one to observe a ΔRI of 0.411 RIU without adjusting optics. Thus, the 450-nm window has roughly an 8-fold larger dynamic range of RI, but the detection limit is proportionately worse. Figure 5a demonstrates that fringing was occurring as far into the blue as 380 nm for concentrated samples. A larger number of fringes allowed better statistics correlating fringe characteristics to samples. Also visible in Figure 5a are variations in how rapidly each reflected spectrum returns to the water baseline. Whereas the narrower window of Figure 4c captured only the rise from the singularity back to baseline, the wider window of Figure 5a shows deviation from the baseline as far out as 750 nm corresponded to the sample concentration.

Spectra of nonabsorbing compounds were distinguished from spectra of absorbers by several characteristics. Nonabsorbing compounds had sharper singularities. The phase of fringes was unaffected by concentration for nonabsorbers but was shifted with the concentration of absorbers. Fringe offset for nonabsorbers was consistently below the water baseline with a gentler negative slope toward the singularity. Fringe amplitude increased more dramatically with concentration for absorbers. The amplitude of the singularity showed greater increase with concentration of nonabsorbers. The calibration curve in Figure 5b was generated using data from Figure 5a. Sharp singularities in spectra of NaCl and other nonabsorbing analytes were useful for easily identifying the singular wavelength. The best-fit line through the points in Figure 5b had an $R^2 = 0.97$, and a slope of 1.8×10^{-3} RIU/nm. The RI discrimination of this calibration was limited only by the resolution and quality of the spectrophotometer that was used. These results were surprisingly close to theory, considering the age and relatively low cost of the Ocean Optics equipment, and confirmed the utility of GLRS to measure sample RI.

A simple separation was used to demonstrate the power of combining chromatographic selectivity with multiwavelength GLRS detection (Figure 6a). A detailed analysis of the data using GLRS theory compared to the experimental results was undertaken.[44] For brevity, a qualitative description of the detailed analysis follows. The analysis confirmed that the Bromocresol green was not a pure compound. Chromatographic peaks are more visible in the total signal chromatogram in Figure 6b. Peaks A and D were most likely trace impurities, present below concentrations necessary to cause fringing. An inspection of the reflection spectra for peaks B and C in Figure 6c indicated that, although the chromatography was insufficient to fully separate all of the compounds, peak B was predominantly salt, and peak C, mostly dye. Characteristics of peak B that indicated a buffer were the following: (1) flat, negatively offset of fringes; (2) sharp singularity; and (3) rapid rise of signal to the red of the singularity. Characteristics of peak C identifying it as an absorber were the following: (1) negative, sloping offset of fringes; (2) broad singularity; and (3) slow return of the signal to baseline to the red of the singularity. On the basis of a 2-nL injection of 5 mM bromocresol green in 125 mM phosphate buffer, the LOD at the detector was roughly 0.1 mM for the pH indicator and 2 mM for the buffer.

A significant power of microfabricated analyzers is the ability to incorporate multiple components into a single device. Traditional transmission absorption spectroscopy was performed simultaneously with light that was transmitted through the same detection volume used for GLRS. Figure 7 shows the simultaneous GLRS and traditional absorbance detection of the three food dyes. Although the combination of chromatographic separation and multiwavelength absorbance detection was sufficient to fully resolve each analyte, GLRS provides complementary information, as was previously demonstrated for the detection of nonabsorbing analytes (Figure 6). A separation efficiency, *N*, of 16 000 was achieved for an unretained dye peak eluting at 12 min. The Red #3 in this experiment was diluted at the detector by a factor of 30, as compared to the 2-nL peak in Figure 4a, and therefore, it did not appear in the GLRS contour plot of Figure 7. Still, the unique response from each detection method allowed positive identification of every analyte.

CONCLUSIONS

Versatile injection strategy and multiwavelength detection made this a broadly applicable analyzer for near-real-time sampling, flow injection analysis or capillary separation, followed by multidimensional detection. The phenomenon of fringing within the wavelength dimension appears to be a new and sensitive attribute of this GLRS configuration that contained additional

(44) Smith, S. A. Doctoral Dissertation, University of Washington, Seattle, WA, 2000, Chapter 6.

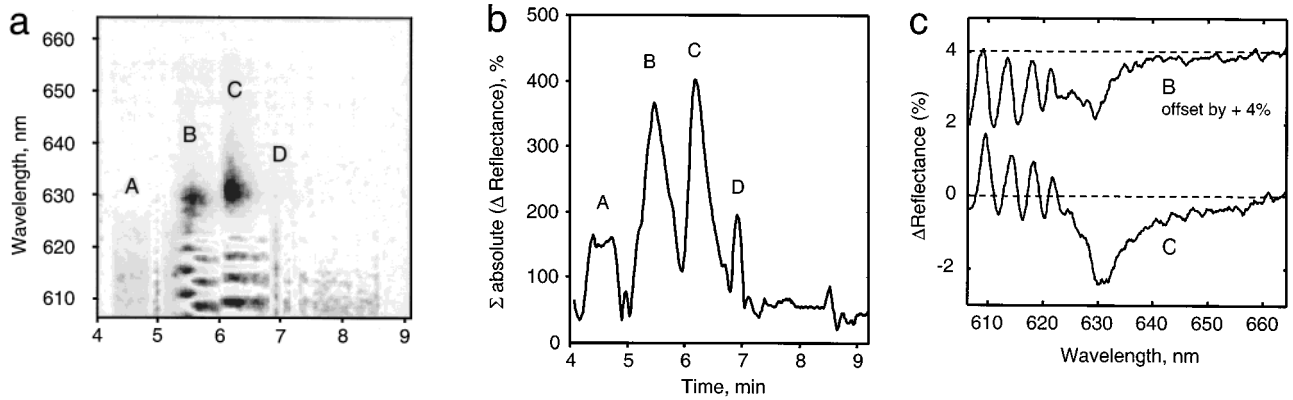

Figure 6. (a) Microchannel separation with GLRS detection. Sample was 5 mM Bromocresol green in 125 mM phosphate buffer, pH 5.9, with 2 nL injected. Mobile phase was deionized water flowing down the separation channel at 10 nL/min. Dimensions of channel were 100 μm × 11 μm × 4.4 cm. Data collected using the McPherson monochromator and a CCD camera. (b) Chromatographic peaks are more clearly seen by summing the absolute values of data along the wavelength axis. (c) Change in reflectance versus water (dotted lines) for chromatographic peaks B and C. Spectrum for peak B was offset by +4% for clarity.

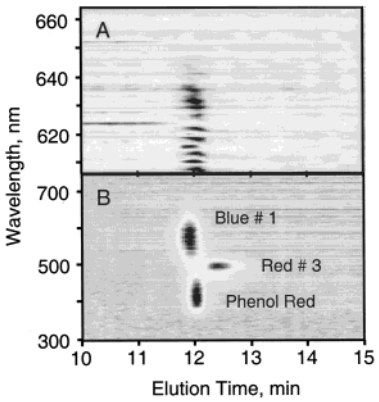

Figure 7. Simultaneous GLRS and absorbance detection of a microchannel separation are shown in contour plots. Sample was 7.3 mM FD&C Blue #1, 3 mM FD&C Red#3, and 3 mM Phenol Red dissolved in water. Mobile phase was 0.5 mM phosphate buffer, pH 7.0, flowing at 20 nL/min. A 3-nL sample was injected into a 100 μm × 10 μm × 23 cm channel. Chromatographic separation and multiwavelength detection were sufficient to positively identify each analyte. Only FD&C Blue #1 and Phenol Red are visible in the GLRS plot (two fringe patterns slightly offset in time). GLRS data collected using the McPherson 270 monochromator and absorbance data collected using an Ocean Optics SD2000 diode-array spectrophotometer.

information. Although the source of fringing was not completely delineated, GLRS spectra showed fringes ending at the singularity, implicating the grating as having an integral role. A further requirement for fringing was detection in a channel that was overfilled by the beam of incident light in the *x* dimension (as defined in Figure 1a and b). Further characterization of the cause of fringes and of the information contained therein is warranted.

The sampling studies demonstrated the value of a parallel plate chromatographic system, clearly showing the advantage of the aspect ratio. The novel injection scheme was shown to produce small, reproducible injections that are needed for an effective microfabricated device, producing a relatively high chromatographic efficiency. These larger injection volumes will create a system with a higher throughput that will decrease the lag time for near-real-time sampling.

The ultimate goal of achieving a truly universal device with on-chip sampling, sample handling, and detection will likely require an improved sampling technique and an array of sensing techniques.[3] Steps toward this end were made in these studies by incorporating multiple detection methods and real-time sampling techniques into a single device. Absorbance, RI, and chromatographic properties of samples were probed, thereby increasing the range of compounds that can be analyzed, as compared to a single detection method. Limits of detection were typically 10^{-4} M, which is adequate for many applications. Increasing the utility of μ-TAS must involve efforts to continue development of inexpensive, universal, and path-length-independent methods of detection and injection techniques that provide very small, controlled, and reproducible injections.

ACKNOWLEDGMENT

We thank the Center for Process Analytical Chemistry (CPAC), a National Science Foundation-initiated University/Industry Cooperative Research Center at the University of Washington, for financial support.

Received for review April 16, 2001. Accepted October 10, 2001.

AC010440O